

ARTICLE

High Resolution Crossed Molecular Beams Study on the $F+HD\rightarrow HF+D$ Reaction at Collision Energy of 5.43–18.73 kJ/mol[†]

Wen-rui Dong, Chun-lei Xiao, Tao Wang, Dong-xu Dai, Xiu-yan Wang, Xue-ming Yang*

State Key Laboratory of Molecular Reaction Dynamics, Dalian Institute of Chemical Physics, Chinese Academy of Sciences, Dalian 116023, China

(Dated: Received on July 8, 2011; Accepted on July 25, 2011)

The dynamics of $F+HD\rightarrow HF+D$ reaction has been studied at ten collision energies ranging from 5.43 kJ/mol to 18.73 kJ/mol using high-resolution H/D atom Rydberg tagging time-of-flight method. Product vibrational and rotational state-resolved differential cross sections have been determined. The intensity of the $HF(v'=2)$ forward products decreases as the collision energy increases, suggesting that the resonance contribution is reduced as the collision energy increases. The forward peak of $HF(v'=3)$ product has also been observed above the threshold of this product channel. Product energy disposals in different degrees of freedom have been analyzed. The collision energy dependence of the HF vibrational product branching was also determined. This work presents a comprehensive dynamic picture of this resonance mediated reaction in a wide collision energy regime, providing a good test ground for theoretical understandings of this interesting reaction at higher collision energies.

Key words: $F+HD\rightarrow HF+D$, Crossed molecular beam, Rydberg tagging, Reactive resonance

I. INTRODUCTION

The $F+H_2$ reaction and its isotopic variants have been extensively studied by experimental and theoretical scientists because of its importance in the development of reaction dynamics. Since the first theoretical predictions of dynamical resonance in the $F+H_2$ reaction [1–3], searching for experimental evidence of reaction resonance has become a central issue in the study of chemical reaction dynamics. Neumark *et al.* performed a landmark crossed-beams experiment on the $F+H_2$ reaction using the universal crossed molecular beams technique [4, 5]. A clear forward scattering peak was observed for the $HF(v'=3)$ product, which was attributed to reaction resonances in this reaction. Furthermore, forward scattering for the $DF(v'=4)$ product from $F+D_2$ as well as the $HF(v'=3)$ product from $F+HD$ was observed [6], consistent with the $F+H_2$ experiment [4].

Exact quantum mechanical (QM) scattering calculations of the $F+H_2$ reaction [7] on the Stark-Werner PES (SW-PES) [8] show that $HF(v'=3)$ forward scattering did not have a clear signature of a reaction resonance. Quasi-classical trajectory (QCT) calculations on the SW surface by Aoiz *et al.* also exhibit forwarding

scattering of $HF(v'=3)$ in the same reaction [9], implying that $HF(v=3)$ forward scattering is probably not related to a quantum resonance. Clearly, the SW-PES is reasonably accurate in describing the transition state region for the $F+H_2$ reaction as revealed in the negative ion photodetachment study of the FH_2^- system [10–12]. Therefore, the assignment of the $HF(v'=3)$ forward scattering to the reaction resonance is certainly questionable.

Liu and coworkers carried out a crossed beam experiment on the $F+HD\rightarrow HF+D$ reaction, and observed a step or a peak in the excitation function at the low collision energy [13, 14], which was attributed to reaction resonance in the $F+HD$ reaction. In addition, Liu and coworkers measured differential cross sections for the same reaction in a wide collision energy range from 1.67 kJ/mol to 18.93 kJ/mol [15, 16], and concluded that at collision energy lower than 5.02 kJ/mol, the reaction proceeds almost exclusively through resonance tunnelling. In the case of the $F+H_2$ reaction, no peak in the excitation function has been observed by Liu and coworkers. In a series of combined experimental and theoretical studies of the $F+H_2$ reaction with full product quantum state resolution in our laboratory, we have observed clear Feibach resonances [17–22]. A new and improved potential energy surface, XXZ-PES was constructed to elucidate the resonance in the reactive system [23].

For the $F+HD\rightarrow HF+D$, we have also performed a series of high resolution crossed molecular beam experiments [24] in the collision energy range of 0.84 kJ/mol

[†]Part of the special issue for “the Chinese Chemical Society’s 12th National Chemical Dynamics Symposium”.

*Author to whom correspondence should be addressed. E-mail: xmyang@dicp.ac.cn

to 5.02 kJ/mol. The isotope effect on Feibach resonances in this system has been clarified by a highly accurate CCSD(T) potential energy surface, XZ-PES. A clear physical picture of reaction resonances in this benchmark system has been well established, which is important in the collision energy region (<6.27 kJ/mol). The dynamics of this benchmark system in the higher collision energy region, however, has received less attention. As mentioned above, Liu and coworkers [15, 16] has performed a detailed crossed study on the F+HD reaction in the higher collision energy range, in addition to the original work by Lee and coworkers [6]. However, both experiments were carried out at relatively lower resolutions. Therefore, it is necessary to reinvestigate the dynamics of the F+HD \rightarrow HF+D reaction at higher collision energies.

In this work, we have carried out a high resolution crossed beam experiment on the F+HD \rightarrow HF+D reaction at collision energies from 5.43 kJ/mol to 18.73 kJ/mol, using the high resolution H-atom Rydberg tagging technique.

II. EXPERIMENTS

Full quantum state resolution crossed molecular beam scattering experiment on the F+H₂ and its isotopic variants has been carried out in our laboratory using the D-atom Rydberg tagging time-of-flight (TOF) technique. The experiment was conducted in a crossed beam apparatus, which has been described in details previously [25]. The double skimmed F atom beam was produced by the double-stage pulse discharge of F₂ (5% in He at 400 kPa). The F atom in the beam was found to be mainly in the ground state F(²P_{3/2}) and only a small amount of the spin-orbit excited F*(²P_{1/2}). The ratio between F and F* was about 10.7, which was determined through vacuum ultraviolet (VUV) synchrotron ionization. In order to have a better resolution of the experiment, the HD beam was obtained by expansion of the neat HD sample through the liquid-nitrogen cooled general pulse valve. At collision energy of 11.20 kJ/mol and above, in order to reach the higher collision energy and also to detect the full angle of the product in the center-of-mass (CM) frame, the HD beam was expanded through the Even-Lavie supersonic pulse valve in room temperature. The rotational distribution of the HD beam is almost all in $j'=0$ for the former and about 88% in $j'=0$, 9% in $j'=1$, and 3% in $j'=2$ for the latter method. The ratio of the rotational distribution was measured using the resonance enhanced multiphoton ionization (REMPI) method. The D-atom product was first excited from the ground state (with principle quantum number $n=1$) to $n=2$ by the 121.6 nm VUV light which is generated by a two-photon resonance ($2\omega_1-\omega_2$) four-wave mixing scheme in a Kr/Ar gas cell. Then the D-atom of $n=2$ was sequentially excited to the high Rydberg state with $n\approx 50$ by the 365 nm light. The

long-lived Rydberg D-atoms fly about 317 mm before they were field-ionized by the electric field applied in front of the microchannel plate (MCP) detector which covers the detectable angle from -45° to 135° , so we can observe the product in full angle from forward to backward in the CM frame. The signal detected by the MCP detector is subsequently amplified by a fast pre-amplifier, and then counted by a multichannel scaler (MCS). One of the molecular beams was rotationable, so we can change the collision energy conveniently by simply altering the crossing angle of the two beams. In this way, we performed experiment at ten collision energies from 5.43 kJ/mol to 18.73 kJ/mol.

III. RESULTS

A. HF product velocity distributions

In this experiment, the TOF spectra of the D atom product at 18 different angles from the F+HD reaction have been measured at ten different collision energies. These TOF spectra were then converted into product velocity distributions. Figure 1 shows the D product velocity distributions at three different scattering angles of forward, backward and sideways, at four typical collision energies. In the first row of Fig.1, three velocity distributions at the collision energy of 5.43 kJ/mol were shown. Clearly, HF($v'=2$) product is the dominant product in all scattering angles at this collision energy. In the forward and the backward direction, the HF($v'=2$) product peaks at $j'=2$; while in the sideways direction it is rotationally much hotter with a peaked distribution at about $j'=10$. HF($v'=1$) product is also present at this collision energy. In the backward direction, the HF($v'=1$) product seems to have a bimodal structure in rotational distribution which peaks at about $j'=4$ and $j'=11$.

At the collision energy of 8.69 kJ/mol, the overall features of the HF($v'=1$) and HF($v'=2$) products are quite similar to that of 5.43 kJ/mol. However, in the forward and backward directions, the HF($v'=1$) and HF($v'=2$) products are more rotationally excited. At this collision energy, the HF($v'=3$) product appears because the collision energy is already above the threshold of this product channel. In the HF($v'=2$) forward direction, in Fig.1(f), no HF($v'=3$) product was detected because of the scattering kinematics at the scattering angle. We have scanned many scattering angles, so the full DCS for the HF($v'=3$) product can still be obtained.

At the collision energy of 12.71 kJ/mol, the rotational distribution of the HF($v'=2$) becomes even hotter as the scattering angle changes from backward to forward direction. The rotational distribution peaks around $j'=5$ in the backward direction, while it reaches its maximum distribution at $j'=13$ in the forward direction. For the HF($v'=1$) product, the rotational distribution peaks around $j'=11$ in the backward direction and becomes a

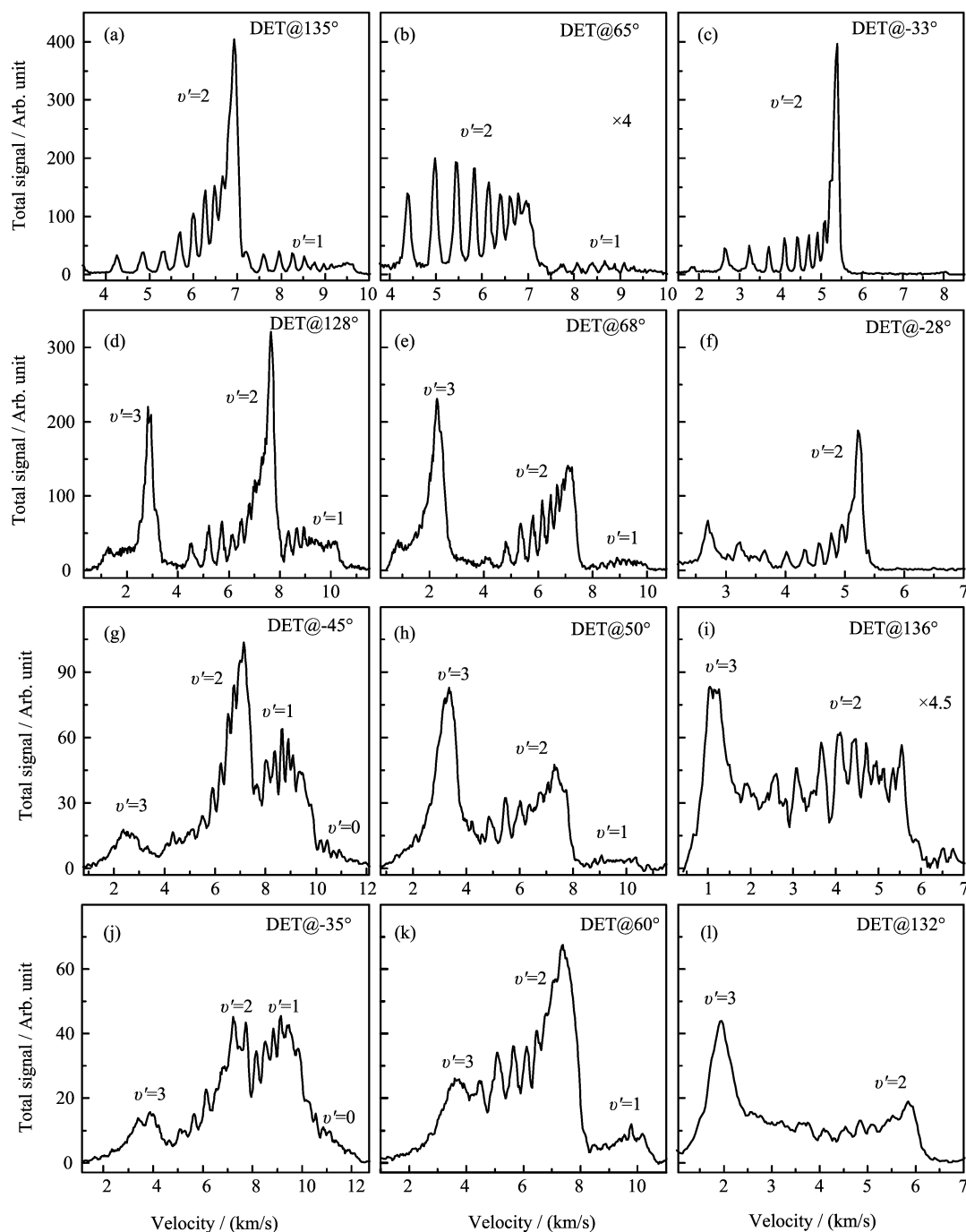


FIG. 1 Velocity spectra of the D-atom product from the F+HD reaction in the backward (left panel), sideway (medium panel), and forward (right panel) direction at four collision energies indicated. Note: the laboratory angles labelled at the two higher collision energies are different from the two lower collision energies because the two beam sources were switched for high collision energy experiments. (a)–(c) 5.43 kJ/mol, (d)–(f) 8.69 kJ/mol, (g)–(i) 12.71 kJ/mol, and (j)–(l) 16.80 kJ/mol.

little cooler when shift to sideway. It is necessary to point out that the resolution is better for the product velocity distributions at collision energies in the range of 5.43–9.95 kJ/mol from which at the collision energies in the range of 11.20–18.73 kJ/mol. In the range of 5.43–9.95 kJ/mol, the data were measured using a

liquid nitrogen cooled HD beam, while in the higher energy region, the experiment was carried out with a room temperature HD beam.

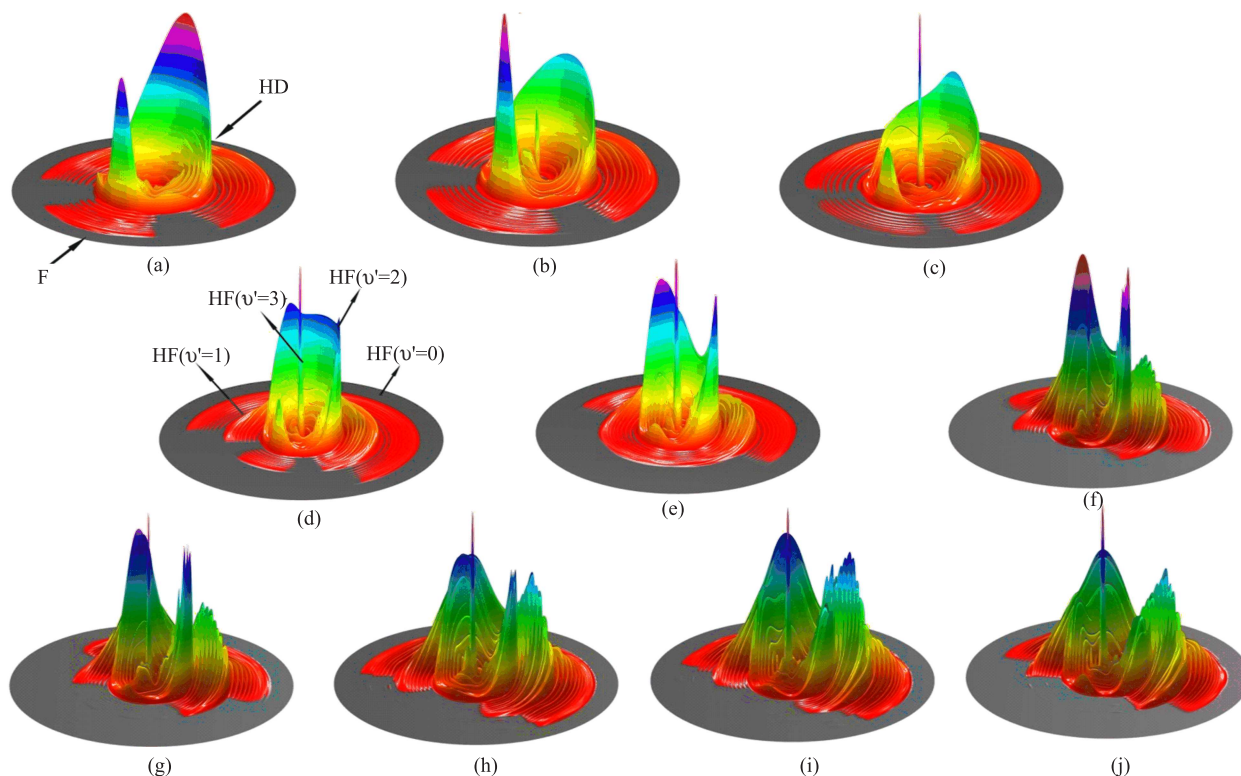


FIG. 2 The experimental 3D contour plots for the product translational energy and angular distributions for the F+HD reaction at various collision energies: 5.43 kJ/mol (a), 6.69 kJ/mol (b), 7.77 kJ/mol (c), 8.69 kJ/mol (d), 9.95 kJ/mol (e), 11.20 kJ/mol (f), 12.70 kJ/mol (g), 14.50 kJ/mol (h), 16.80 kJ/mol (i), 18.73 kJ/mol (j).

B. Product differential cross sections

From the fitting velocity distributions, as shown in Fig.1, rovibrational state distributions of the HF product can be obtained at different CM scattering angles for any specific collision energies. From these quantum state specific differential cross sections, we can then construct a three dimensional (3D) DCS contour for the F+HD→HF+D reaction at each collision energy studied in this work. Figure 2 shows the 3D DCS contour at 10 collision energies ranging from 5.43 kJ/mol to 18.73 kJ/mol. In the 3D DCS contours, each ring corresponds to a specific rovibrational state of HF. Prominent clustered structures can be assigned, from the innermost one, to HF ($v'=3, 2, 1, 0$). Figure 2(a) shows the 3D DCS contours at the collision energy of 5.43 kJ/mol, no HF($v'=3$) product is observed because the collision energy is below the threshold of this channel, which is calculated to be about 5.60 kJ/mol, slightly different from the earlier value of 4.85 kJ/mol estimated by Liu and workers [15, 16]. In their analyses, the exothermicity of the title reaction is 130.63 kJ/mol, and the formation of the HF($v'=3$) needs 135.47 kJ/mol [15] while in our simulation the two energies are 130.33 and 135.93 kJ/mol, respectively. At all the collision energies that above the threshold of HF($v'=3$), the forward peaks of this channel are sig-

nificant. As the collision energy increased, the backward product of HF($v'=2$) shifts towards sideway while the forward product decreases after it reaches maximum of 6.69 kJ/mol. At the five lower collision energies, the HF($v'=1$) product have small distribution in the forward direction although the product flux of this channel is dominated in the backward. The branch ratio of the HF($v'=1$) product rise with collision energy and becomes the most populated state at collision energies higher than 14.80 kJ/mol. Since its onset at 7.65 kJ/mol, the HF($v'=0$) product branching also increases as the collision energy goes up.

Extensive study on this reaction has been done by Liu and coworkers [15, 16]. In their previous experiment, they have also measured product 3D DCS at many collision energies. We have made some comparisons between their results and our results, it seems there are some noticeable differences. The most obvious difference is around 8.36 kJ/mol. Liu's results show a prominent forward peak of HF($v'=2$) while only a little product flux in the backward direction, while our experiment indicates that most of the HF($v'=2$) product appears at the backward direction and only a narrow peak is present at the forward direction at 8.69 kJ/mol. This is probably hard to attribute to the small difference in the collision energy (0.33 kJ/mol). These differences could be caused by the different experimental

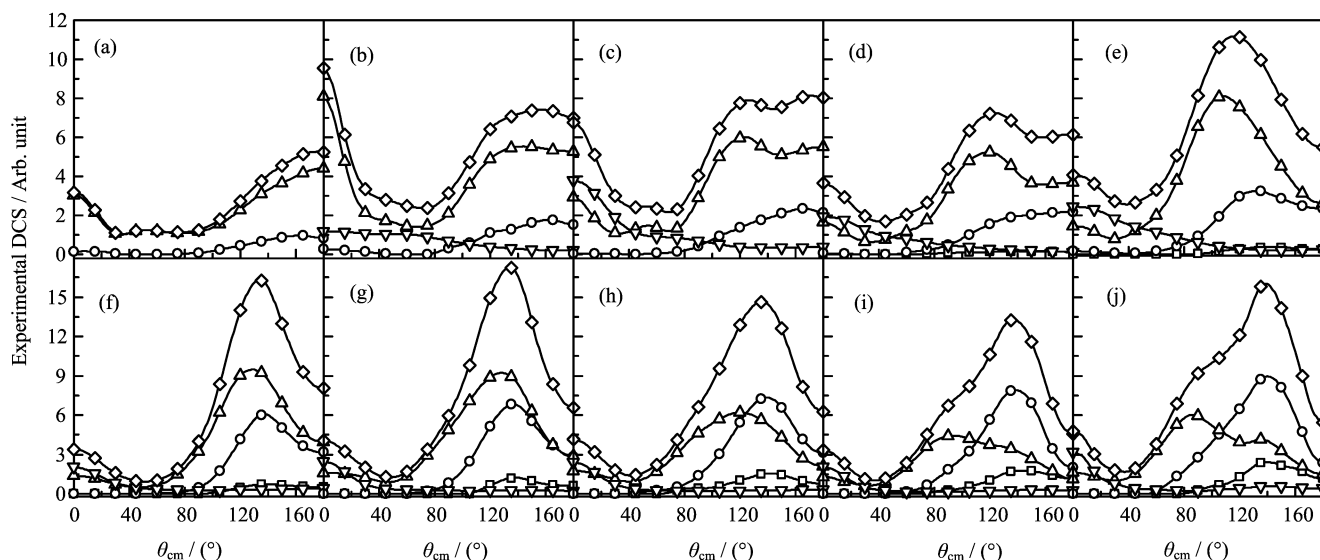


FIG. 3 Total and vibrational state-resolved CM DCS at ten collision energies: 5.43 kJ/mol (a), 6.69 kJ/mol (b), 7.77 kJ/mol (c), 8.69 kJ/mol (d), 9.95 kJ/mol (e), 11.20 kJ/mol (f), 12.70 kJ/mol (g), 14.50 kJ/mol (h), 16.80 kJ/mol (i), and 18.73 kJ/mol (j). “□” $v'=0$, “o” $v'=1$, “△” $v'=2$, “▽” $v'=3$, and “◇” total.

conditions. In our experiment, the HD molecules in the beam are nearly all distributed in the $j'=0$ state, while in Liu's experiment, there is a significant amount of the $j'=1$ state [15, 16]. The molecular beam conditions are also slightly different in the two sets of experiment.

The 3D DCS contours in Fig. 2 provide a rather complete view of the reaction dynamics change in the F+HD→HF+D reaction as the collision energy varies from 5.43 kJ/mol to 18.73 kJ/mol. By integrating the rotational populations for each vibrational state of the HF product at specific scattering angles, we can determine the angular distribution of the HF product on $v'=0, 1, 2, 3$ vibrational states. Figure 3 shows the angular distributions of vibrational state specific HF products from F+HD→HF+D at the ten collision energies studied in this experiment. From these results, it is interesting to notice that the angular distributions for different HF vibrational state products are very different. In the forward direction, the total scattering flux of the title reaction are mainly from the HF($v'=2$) and HF($v'=3$) products throughout the collision energy region we have studied. The contribution of the HF($v'=2$) and HF($v'=3$) is comparable in the forward direction, which seems to be in conflict with the 3D DCS in Fig. 2. This phenomenon is due to the fact that the rotational distribution of the HF($v'=3$) is much narrower than HF($v'=2$) in the forward direction. As the collision energy increased, the HF($v'=2$) have more sideways contribution while the HF($v'=1$) have more backward scattered contribution.

By integrating the angular distributions for specific vibrational state HF product at different collision energies, the dependence of the relative vibrational state branchings of the HF product was determined and is

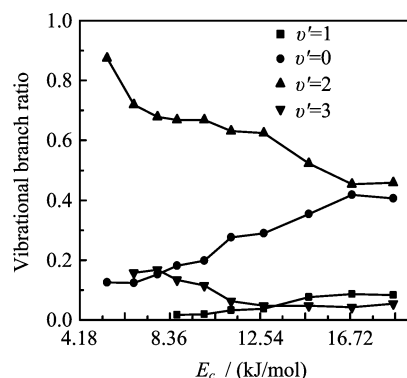


FIG. 4 Product vibrational branch ratio change with collision energy.

shown in Fig. 4. Interestingly, the relative branching of HF($v'=0$) and HF($v'=1$) products increases as the collision energy increases, while that of HF($v'=2$) and HF($v'=3$) decreases as the collision energy increases. The dynamical origin of these variations is, however, not immediately clear.

C. Product energy disposals

By fitting the TOF spectra of the D atom product, we have obtained detailed rotational and vibrational state distributions of the HF product at different collision energies. Using this information, the product energy partition in translation, vibration, and rotation in this reaction can be determined. Figure 5 shows the angular dependence of the energy disposal in the rotational $\langle f_r \rangle$, vibrational $\langle f_v \rangle$, and translational $\langle f_t \rangle$ energy. The ro-

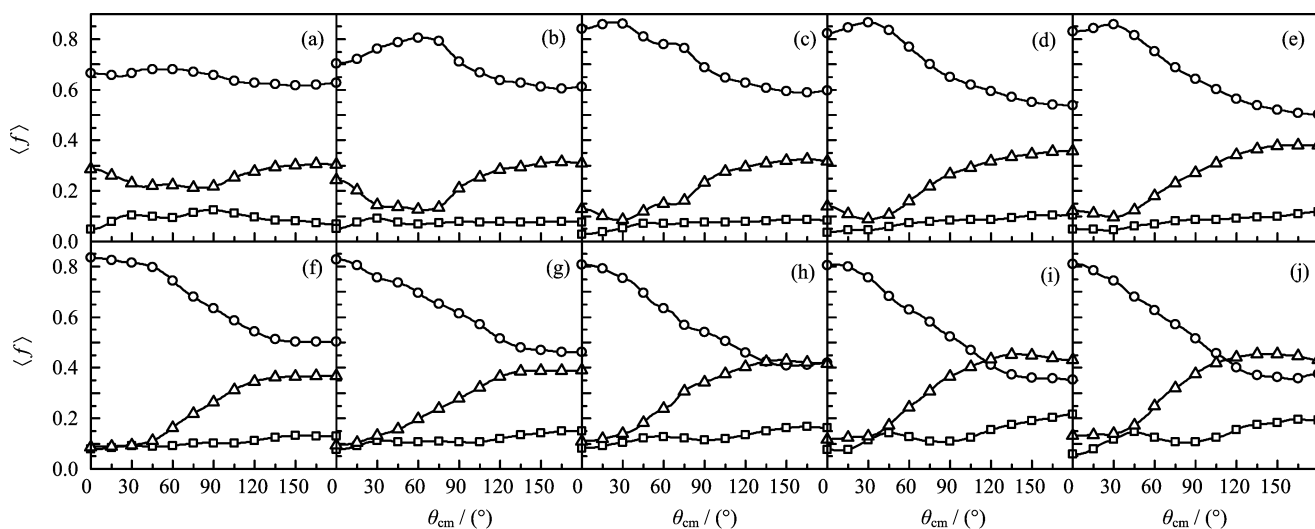


FIG. 5 Angular dependence of the product energy disposal. The corresponding collision energies are: 5.43 kJ/mol (a), 6.69 kJ/mol (b), 7.77 kJ/mol (c), 8.69 kJ/mol (d), 9.95 kJ/mol (e), 11.20 kJ/mol (f), 12.70 kJ/mol (g), 14.50 kJ/mol (h), 16.80 kJ/mol (i), and 18.73 kJ/mol (j). “□” $\langle f_r \rangle$, “○” $\langle f_v \rangle$, and “△” $\langle f_t \rangle$.

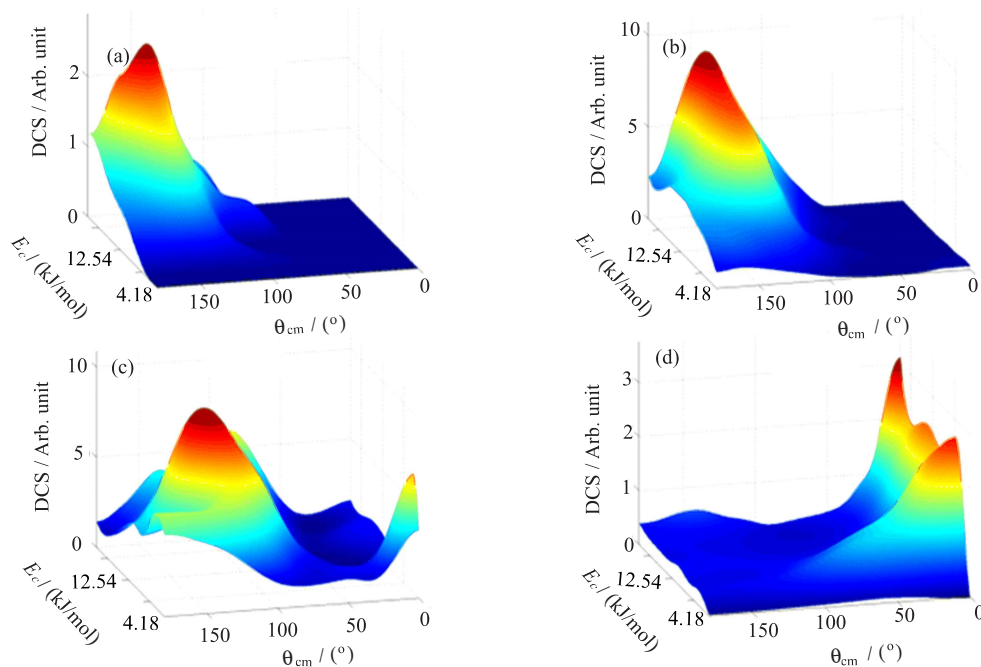


FIG. 6 Vibrational-resolved collision energy-dependent DCS. (a) $v=0$, (b) $v=1$, (c) $v=2$, and (d) $v=3$.

tational energy disposal is not strongly dependent on the scattering angles in the whole collision energy region studied in this work. As the collision energy increases, the $\langle f_r \rangle$ only goes up slowly as the scattering angle changes from forward to backward. At most collision energies, $\langle f_v \rangle$ goes down as the scattering direction changes from forward to backward; while $\langle f_t \rangle$ goes up. In comparison with Ref.[16], the two sets of results at collision energies higher than 12.54 kJ/mol are quite similar.

D. Collision energy dependent differential cross sections

The reaction resonance in the $F+HD \rightarrow HF+D$ reaction at collision energies lower than 5.43 kJ/mol plays a dominant role [24, 26–28]. One main feature of the resonance is the forward scattering of the HF product. It is therefore interesting to see how angular distribution of different HF vibrational state product changes with the collision energy larger than 5.43 kJ/mol and how the forward and backward scattering HF products

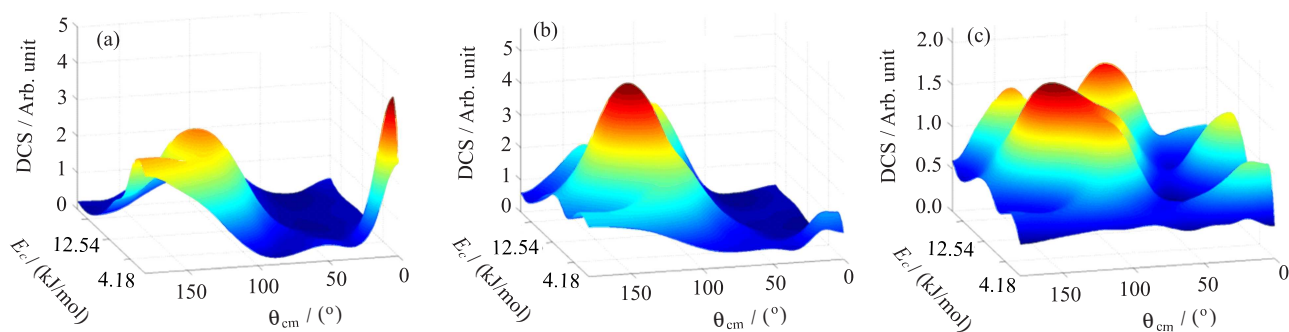


FIG. 7 Collision energy dependent DCS of the HF($v'=2$), $j'=0-4$ (a), $5-8$ (b), and $9-13$ (c), respectively.

vary with the collision energy. In the experiment, we have measured the backward scattering HF signals at different collision energies, therefore all DCS can be connected relatively. Figure 6 shows the collision energy-dependent DCS for different HF vibrational state product. For HF($v'=3$), the product is dominantly forward scattered with oscillatory structures as the collision energy changes. The forward scattering product at high collision energy for the $v'=3$ HF product is very interesting. Whether this is related to the Feshbach resonances [26, 27, 29] remains to be investigated. The HF($v'=2$) product is very different from HF($v'=3$), it only shows a forward peak at collision energies below 8.36 kJ/mol. This forward peak is very likely related to the Feshbach resonances. At higher collision energies, the HF($v'=2$) product are mainly scattered in the backward sideway direction, which is probably due to direct reaction mechanism [16, 26, 27, 29]. For HF($v'=1$), there are some small forward scattering signal, as collision energy increases, this forward scattering signal disappeared. The forward scattered signal at low collision energy should also be related to the Feshbach resonance at the low collision energies. At higher collision, the product is dominantly backward scattering, which is likely due to the direct reaction mechanism.

The HF($v'=2$) products at all the collision energies are fully or at least partially rovibrational state resolved, therefore, how resonance affects product rotational distribution can be investigated in detail. In Fig.7, the collision energy dependent DCS of HF($v'=2$) for three different rotational ranges: $j'=0-4$, $5-8$, $9-13$, are shown. It is very interesting that different HF($v'=2$) rotational states show very different angular distributions and energy dependence. The HF($v'=2$) product in the $j'=0-4$ range shows the biggest forward scattering at the low collision energy, and it goes down quickly as the collision energy increases. The HF($v'=2$) product in the $j'=5-8$ range shows similar behavior. For the HF($v'=2$) product in the $j'=9-13$ range, the forward scattering signal goes up and down twice, which is very intriguing. Theoretical studies for this behavior is clearly needed to explain this interesting phenomenon.

IV. CONCLUSION

In this work, we performed high resolution crossed molecular beam experiment on the F+HD reaction at ten collision energies ranging from 5.43 kJ/mol to 18.73 kJ/mol using the D-atom Rydberg tagging time-of-flight technique. Quantum state resolved differential cross sections have been measured. From the product DCS, we observed the backward product of the HF($v'=2$) shift to the sideway as the collision energy increased, while the forward product lose their intensity gradually in this process. For the HF($v'=3$) product, the forward scatterings are always dominant once the collision energy is above the threshold of this channel. The HF($v'=0$) and HF($v'=1$) products are mostly scattered in the backward direction with only a small amount of HF($v'=1$) in the forward direction. We have also compared with the results of the crossed beams experiment in Ref.[16]. There are clear differences between our results and those of Lee *et al.* [16]. This is probably due to the different experimental conditions in the two experiments, as well as the different detection method.

Vibrational branchings of the HF product have been determined in the current experiment. As the collision energy increases, the relative population of the HF($v'=0$) and HF($v'=1$) product increases, while that of HF($v'=2$) and HF($v'=3$) decreases. In the product energy disposal, $\langle f_r \rangle$ goes up gradually from forward to backward because the main product in the backward direction are rotationally hotter than that of the forward one averagely. The $\langle f_v \rangle$ increases with shift from sideway to the forward direction. For the HF($v'=2$) product at collision energies lower than 8.36 kJ/mol, forward scattering are mostly low j' product, while at higher collision energies higher rotational excitation in HF($v'=2$) is observed in the forward scattering. This set of dynamical results for the F+HD→HF+D reaction is quite complete and it provides a good testing ground for theoretical understanding of the interesting dynamics at the high collision energies for this benchmark system.

V. ACKNOWLEDGMENTS

This work was supported by the Chinese Academy of Sciences, the National Natural Science Foundation of China, and the Ministry of Science and Technology of China.

- [1] G. C. Schatz, J. M. Bowman, and A. Kuppermann, *J. Chem. Phys.* **63**, 674 (1975).
- [2] G. C. Schatz, J. M. Bowman, and A. Kuppermann, *J. Chem. Phys.* **63**, 685 (1975).
- [3] S. F. Wu, B. R. Johnson, and R. D. Levine, *Mol. Phys.* **25**, 839 (1973).
- [4] D. M. Neumark, A. M. Wodtke, G. N. Robinson, C. C. Hayden, and Y. T. Lee, *Phys. Rev. Lett.* **53**, 226 (1984).
- [5] D. M. Neumark, A. M. Wodtke, G. N. Robinson, C. C. Hayden, and Y. T. Lee, *J. Chem. Phys.* **82**, 3045 (1985).
- [6] D. M. Neumark, A. M. Wodtke, G. N. Robinson, C. C. Hayden, K. Shobatake, R. K. Sparks, T. P. Schafer, and Y. T. Lee, *J. Chem. Phys.* **82**, 3067 (1985).
- [7] J. F. Castillo, D. E. Manolopoulos, K. Stark, and H. J. Werner, *J. Chem. Phys.* **104**, 6531 (1996).
- [8] K. Stark and H. J. Werner, *J. Chem. Phys.* **104**, 6515 (1996).
- [9] F. J. Aoiz, L. Banares, V. J. Herrero, V. S. Rabanos, K. Stark, and H. J. Werner, *Chem. Phys. Lett.* **223**, 215 (1994).
- [10] A. Weaver and D. M. Neumark, *Faraday Discuss.* **91**, 5 (1991).
- [11] S. E. Bradforth, D. W. Arnold, D. M. Neumark, and D. E. Manolopoulos, *J. Chem. Phys.* **99**, 6345 (1993).
- [12] D. E. Manolopoulos, K. Stark, H. J. Werner, D. W. Arnold, S. E. Bradforth, and D. M. Neumark, *Science* **262**, 1852 (1993).
- [13] Y. T. Hsu, K. Liu, L. A. Pederson, and G. C. Schatz, *J. Chem. Phys.* **101**, 7921 (1999).
- [14] J. H. Wang, Y. T. Hsu, and K. Liu, *J. Chem. Phys.* **101**, 6593 (1997).
- [15] S. H. Lee, F. Dong, and K. Liu, *J. Chem. Phys.* **116**, 7839 (2002).
- [16] S. H. Lee, F. Dong, and K. Liu, *J. Chem. Phys.* **125**, 133106 (2006).
- [17] M. H. Qiu, Z. F. Ren, L. Che, D. X. Dai, S. A. Harich, X. Y. Wang, X. M. Yang, C. X. Xu, D. Q. Xie, M. Gustafsson, R. T. Skodje, Z. G. Sun, and D. H. Zhang, *Science* **311**, 1440 (2006).
- [18] M. H. Qiu, Z. F. Ren, L. Che, D. X. Dai, S. A. Harich, X. Y. Wang, and X. M. Yang, *Chin. J. Chem. Phys.* **19**, 93 (2006).
- [19] L. Che, Z. F. Ren, X. G. Wang, W. R. Dong, D. X. Dai, X. Y. Wang, D. H. Zhang, X. M. Yang, L. S. Sheng, G. L. Li, H. J. Werner, F. Lique, and M. H. Alexander, *Science* **317**, 1061 (2007).
- [20] Z. F. Ren, L. Che, M. H. Qiu, X. G. Wang, D. X. Dai, S. A. Harich, X. Y. Wang, X. M. Yang, C. X. Xu, D. Q. Xie, Z. G. Sun, and D. H. Zhang, *J. Chem. Phys.* **125**, 151102 (2006).
- [21] X. G. Wang, W. R. Dong, M. H. Qiu, Z. F. Ren, L. Che, D. X. Dai, X. Y. Wang, X. M. Yang, Z. G. Sun, B. N. Fu, S. Y. Lee, X. Xu, and D. H. Zhang, *Proc. Natl. Acad. Sci. USA* **105**, 6227 (2008).
- [22] W. R. Dong, C. L. Xiao, T. Wang, D. X. Dai, X. M. Yang, and D. H. Zhang, *Science* **327**, 1501 (2010).
- [23] C. Xu, D. Xie, and D. H. Zhang, *Chin. J. Chem. Phys.* **19**, 96 (2006).
- [24] Z. F. Ren, L. Che, M. H. Qiu, X. A. Wang, W. R. Dong, D. X. Dai, X. Y. Wang, X. M. Yang, Z. G. Sun, B. Fu, S. Y. Lee, X. Xu, and D. H. Zhang, *Proc. Natl. Acad. Sci. USA* **105**, 12662 (2008).
- [25] M. H. Qiu, L. Che, Z. F. Ren, D. X. Dai, X. Y. Wang, and X. M. Yang, *Rev. Sci. Instrum.* **76**, 016102 (2005).
- [26] R. T. Skodje, D. Skouteris, D. E. Manolopoulos, S. H. Lee, F. Dong, and K. Liu, *J. Chem. Phys.* **112**, 4536 (2000).
- [27] R. T. Skodje, D. Skouteris, D. E. Manolopoulos, S. H. Lee, F. Dong, and K. Liu, *Phys. Rev. Lett.* **85**, 1206 (2000).
- [28] F. Dong, S. H. Lee, and K. Liu, *J. Chem. Phys.* **113**, 3633 (2000).
- [29] S. H. Lee, F. Dong, and K. Liu, *Faraday Discuss.* **127**, 49 (2004).